Robust detection of incipient faults in VSI-fed induction motors using quality control charts.

L. A. Garcia-Escudero, O. Duque-Perez, M. Fernandez-Temprano and D. Morinigo-Sotelo, *Member, IEEE*

Abstract—. **A considerable amount of papers have been published in recent years proposing supervised classifiers to diagnose the health of a machine. The usual procedure with these classifiers is to train them using data acquired through controlled experiments, expecting them to perform well on new data, classifying correctly the condition of a motor. But, obviously, the new motor to be diagnosed cannot be the same that has been used during the training process; it may be a motor with different characteristics and fed from a completely different source. These different conditions between the training process and the testing one can deeply influence the diagnosis. To avoid these drawbacks, in this paper a new method is proposed which is based on robust statistical techniques applied in Quality Control applications. The proposed method is based on the online diagnosis of the operating motor and can detect deviations from the normal operational conditions. A robust approach has been implemented using high-breakdown statistical techniques which can reliably detect anomalous data that often cause an unexpected overestimation of the data variability, reducing the ability of standard procedures to detect faulty conditions in earlier stages. A case study is presented to prove the validity of the proposed approach. Motors of different characteristics, fed from the power line and several different inverters, are tested. Three different fault conditions are provoked, broken bar, a faulty bearing and mixed eccentricity. Experimental results prove that the proposed approach can detect incipient faults.**

Index Terms— **Diagnostic expert systems induction motors, maintenance, monitoring, quality control.**

I. INTRODUCTION

Condition monitoring of induction motors is an ongoing field of research since they account for over 80% of energy conversion in industrial and commercial sectors. An adequate warning of incipient faults via condition monitoring has important advantages such as prevention of costly shutdowns, providing sufficient time for controlled shutdown of the process, reducing the costs of outage time and repairs, diagnosing present maintenance needs, scheduling future preventive maintenance and providing safer operation of the motors Therefore, the availability of a method capable of detecting incipient faults is of great interest.

Moreover, nowadays there is a great amount of motors that are fed by Voltage Source Inverters (VSI). Consequently a practical condition monitoring scheme must have the ability to detect a faulty machine independently of the power source.

Nevertheless, as it has been widely reported, detection and diagnosis are more challenging for VSI-fed motors due to the rise in noise, dynamically changing excitation frequency [1-3], the fact that the field harmonics amplitude is affected by the supply voltage, particularly when speed control is based on voltage regulation, keeping constant the voltage/frequency ratio [4], and that harmonic content depends strongly on the used technique for the control of the inverter and the chosen switching frequencies [5].

One of the most active fields in this area is the application of Machine Learning techniques to the automatic detection of faulty motors with the aim of improving the reliability and efficiency of the diagnosis. A considerable amount of papers have been published in recent years proposing supervised classifiers to diagnose the health of the machine. These classifiers provide a function (linear or non-linear depending on the chosen classifier) to separate the data into two or more classes. This function is inferred from a set of training examples characterized as a labeled training data, with the labels corresponding to the different motor conditions to diagnose.

One of the most popular tools in diagnosis is the Artificial Neural Networks. They have been extensively used to monitor broken bars [6-20], eccentricity [7],[9][14-25], and bearing related faults [10][14-18][20][26-34]. Similarly, the use of Support Vector Machines to diagnose motors faults has been widely reported in literature: for broken bars [6] [35-39], bearings [31][37][40-50] and eccentricity [37], [44].

Other Machine Learning tools have also been reported in literature. K-nearest neighbors has been applied to diagnose broken bars [6] and bearing faults [51]. [52] uses a supervised fuzzy-neighborhood density-based clustering to diagnose bearing faults. [53] applies random forest algorithm and C4.5 decision tree to ball bearing fault diagnosis. In [54], bagging, boosting and stacking methods are implemented to classify eccentricity, broken bars and bearings faults via simulation. In [55], broken bars and bearings faults are diagnosed with Common Vector Approach. A hidden Markov model is applied in [56] to diagnose broken bars, in [57] to bearings faults too and in [58] is combined with a Naïve Bayesian modeling. Decision Trees are used in [53], [59] to bearing faults and in [60] are combined with Fuzzy Min–Max (FMM) neural networks to comprising a hybrid intelligent model to diagnose eccentricity.

Some applications of unsupervised learning techniques to diagnose bearing related faults have also been reported. In these

L.A. Garcia-Escudero and M. Fernandez-Temprano are with the Department of Statistics and Operational Research at E.I.I., University of Valladolid, Spain (e-mails: lagarcia@eio.uva.es, miguelaf@eio.uva.es).

Daniel Morinigo-Sotelo and Oscar Duque-Perez are with the Department of Electrical Engineering at E.I.I., University of Valladolid, Spain (e-mails: daniel.morinigo@eii.uva.es, oscar.duque@eii.uva.es).

cases the data are unlabeled and the procedure tries to find hidden structure from the data. In [61] a K-means clustering approach is proposed while in [62] a weighted local and global regressive mapping algorithm is proposed and compared with other unsupervised learning algorithms, such as locality preserving projection, Isomap, principal component analysis, and Sammon mapping.

The above methods are attractive although they require an initial training phase that is critical for optimal operation. The training phase requires a large set of examples and may be misleading or produce results limited to a set of systems [63]. The usual procedure with these classifiers is to train them using data acquired through controlled experiments. The motor is run in its healthy state and then is taken to a faulty condition (or several intermediate conditions). Once the classifier has been trained with these data, it is expected to perform well on new data and then to correctly classify the condition of a motor. But, obviously, the new motor to be diagnosed cannot be the same that has been used during the training process; it may be a motor with different characteristics and fed from a completely different source. These different conditions between the training process and the testing one can deeply influence the diagnosis.

To avoid these drawbacks, in this paper a new method is proposed which is based on statistical techniques applied in Quality Control applications. The proposed method is based on the online diagnosis of the operating motor and it can detect deviations from the normal operational conditions.

Throughout continuous monitoring of the motor, data can be acquired that correspond to abnormal conditions that do not reflect a faulty condition but other situations such as measurement or acquisition errors. These anomalous data often cause an unexpected overestimation of the data variability. As a consequence, this overestimation reduces the ability of standard (non-robust) procedure to detect faulty conditions in earlier stages. To avoid it, a robust approach has been implemented using high-breakdown statistical techniques which can reliable detect outliers in the data.

The proposed technique uses a multiresolution technique based on wavelet functions to detect significant fault signatures in the spectrum and, then, a Quality Control approach based on robust multivariate control charts using Hotelling's T-square test is applied to detect a progressive deterioration of the motor condition.

The fault signatures use to diagnose induction motors is explained in Section II, while in Sections III and IV the statistical technique proposed is exposed and applied to a case-study in Section V.

II. FAULT SIGNATURES

The proposed methodology to diagnose faulty induction motors can take advantage of any fault signature among all that have been proposed in bibliography. Hence, it can be used in any motor running condition, in stationary or non-stationary regime, as long as a measurable quantity can be extracted. Moreover, the signatures can be extracted from any physical signal acquired from the running motor, that is, stator current, vibration signal, axial flux, torque, …, in frequency domain, time domain or time-frequency-domain [64]. The signatures

can be mixed independently of the regime or signal where they have been extracted.

There is only one practical limitation on the number of signatures to be used. This limitation is related to the calculation of the covariance matrix of the signatures and it is inherently related to the number of tests that have been performed on the motor. The greater the number of tests, the greater the number of features that can be selected. Nevertheless, the use of features that do not contribute to explain the variability of the response variable (the motor condition) can disturb the performance of the diagnosis procedure. Hence, a feature selection can be advisable using any available procedure. ANOVA [65] or a dimension reduction technique such as Principal Component Analysis [66] can be used to estimate the variability of the response explained by the feature

In the case study analysed in Section V, stator current is the signal measured and processed. The features are extracted in the frequency domain using Fast Fourier Transform (FFT) to analyse the stator current during a steady state operation of the motor.

In these conditions, the characteristic fault frequencies are well-known. In the case study shown in section V, three different faults are analysed: broken bars, mixed eccentricity and bearing faults.

When the motor is supplied by a solid-state inverter, line current will contain time harmonics, which will modify the amplitude of existing harmonics or will generate new airgap spatial ones. Therefore, in the case of cage asymmetry and non-sinusoidal voltage supply, fault signatures are identified as sidebands around the frequencies of time-harmonics of line current, at frequencies given by (1)

$$f_{bb} = (k \pm 2ns)f_1 \qquad (1)$$

where k is the order of the line current time harmonics, s is the motor slip, f_1 is the main frequency and n is any positive integer.

In the case of a bearing-related fault, since ball bearings support the rotor, any bearing defect will produce a radial motion between the rotor and stator of the machine, causing the machine air gap to vary in a manner that can be described by a combination of rotating eccentricities moving in both directions, [67]. Therefore, a faulty bearing can be diagnosed observing the sidebands around the stator current harmonics due to the frequency power converter at frequencies given by (2)

$$f_{brn} = \left[k \pm nq\frac{(1-s)}{p} \right]f_1 \qquad (2)$$

where p is the number of pair of poles and q depends on the kind of bearing fault and on the characteristics on the bearing (number of balls, ball diameter, ball pitch diameter respectively, and contact angle of the ball with the races) [68].

For mixed eccentricity, in VSI-fed motors, the fault frequencies are observed as sideband pairs around principal current harmonics introduced by the power supply, situated at a distance equal to the mechanical rotation frequency, according to (3).

$$f_{ecc} = k f_1 \pm n f_r. \qquad (3)$$

where

$$f_r = \left[\frac{(1-s)}{p} \right]f_1 \qquad (4)$$

III. QUALITY CONTROL CHARTS

Control chart is surely the most widely used tool of the "magnificent seven" tools [69] of Statistical Process Control (SPC). In the recent literature of SPC it is common to distinguish two phases in the development and implementation of control charts. Phase I, sometimes called Initial Study (e.g. [70]), is primarily used, according to [69], to bring the process to a state of statistical control, analyzing historical process data to establish an initial set of in-control data that contains no outliers [71]. This analysis may require several iterations to detect these points and correct its causes. In the multivariate context we are considering, the construction of this initial in-control data set is more difficult as some additional problems not arising in the univariate context may appear such as, among others, the determination of the proper functional form of the variables involved, the possible appearance of multicollinearity which would lead to an unstable estimate of the covariance matrix of the variables and the determination of multivariate outliers. A full description of these problems and the ways of dealing with them can be found in [72].

Once the in-control data set has been established, the in-control process parameters estimated and the control limits determined, in Phase II, also called Control to Standard, the process is monitored comparing the successive observed values of the process with the control limits thus detecting when the process goes out of control. In the multivariate context the interpretation of out-of-control signals is also more involved than in the univariate case as the reason for this signal may come, for example, from one or more of the variables considered or from departures from the correlation structure coming from the in-control data set. Several methods have been developed to interpret out-of-control signals such as, for example, the MYT decomposition [73] or Hawkings method based on regression-adjustments [74]. A comparative study of these classical methods can be found in [75]. More recently, classification techniques, such as, among others, neural networks or decision trees, are being used to analyze and interpret these signals. [76-77] contain a description of these methods together with a comparison among them with boosting [78] showing the best performance according to [77].

IV. ROBUST QUALITY CONTROL CHARTS

As previously commented, two phases may be distinguished in quality control charts.

Phase I: Assume that $x_i = (x_{i1}, \ldots, x_{ip})'$, $i=1,\ldots,n$ are the n observations taken from the in-control situation after measuring key p features (e.g., p seemingly important features extracted from the frequency domain). It is quite common to use the Hotelling's T2 chart as a Quality Control tool. This chart is based on monitoring the squared Mahalanobis distance, which measures the distance of x_i to the overall sample mean vector $\bar{x}$ and takes into account the covariance structure through the sample covariance matrix S. In other words, this Hotelling's T2 chart is based on the monitoring of:

$$T_i^2 = (x_i - \bar{x})'S^{-1}(x_i - \bar{x}), i = 1, \ldots, n. \qquad (4)$$

When monitoring these quantities, the following upper control limit (UCL) is often applied:

$$UCL = \frac{(n-1)^2}{n} B_{\alpha;\frac{p}{2},\frac{n-p-1}{2}}, \qquad (5)$$

where $B_{\alpha;u,v}$ is the (1-α) percentile of the beta distribution with parameters u and v. The use of these limits guarantees a probability α of false alarm for each observation when assuming multivariate normality for the observations.

However, it is also well-known that the sample mean $\bar{x}$ and the sample covariance matrix S can be heavily influenced even by a small amount of outlying observations. Unfortunately, unexpected outliers are likely to appear in our in-control sample of observations given the high signal-to-noise ratios frequently present in the spectrum which may result in occasional problems in the determination of their monitored peaks. Moreover, multiple outliers tend to inflate the classical variance-covariance estimates in such a way that they can "mask" each other. This problem is often known as "masking effect" [79]. The overestimation of the scatter of the in-control data causes that all the T_i^2 in (4) simultaneously shrink. Therefore, it may be wrongly decided to use all the observations to estimate the in-control parameters. Consequently, there will be problems in Phase II for detecting out-of-control cases.

To overcome this trouble with outlying observations, it was suggested to replace the sample mean and the sample covariance matrix S by robust location and scatter matrix estimates [80-83]. For instance, the minimum covariance determinant (MCD) and the minimum volume ellipsoid (MVE) estimators [80] can be used.

Focusing on the MCD as high-breakdown procedure, this estimator can be applied by resorting to *covMcd* function within the robustbase package available at the CRAN repository (http://www.cran.r-project.org) This package returns robust location and scatter matrix estimators denoted, respectively, as $\overline{x_{MCD}}$ and S_{MCD}.

Using these estimators, the robustified Hotelling's T2 distances can be defined as:

$$T_{i,MCD}^2 = (x_i - \overline{x_{MCD}})'S_{MCD}^{-1}(x_i - \overline{x_{MCD}}) \ , i = 1, \ldots, n. \quad (6)$$

The distribution of this robustified T^2 statistics does not admit a closed explicit form but, in order to establish upper control limit, simulations can be used [81].

Fig. 1 shows how traditional Mahalanobis distances are inflated due to the presence of a few outlying observations and, thus, the classical tolerance ellipsoids (i.e., the use of traditional Mahalanobis distances) can fail at detecting other clearly anomalous observations. For instance, traditional (non-robust) Hotelling's T2 chart can detect the 3 most clear outliers in the "Broken bar diagnosis" example in the following Section. However, this method fails at detecting other outlying observations that remain hidden due to the "masking" effect. On the other hand, we can detect these clear 3 outlying observations together with many other outlying ones (see Fig. 2 top) when using the robustified T^2 statistics and a robust Hotelling's T2 chart.

Therefore, the proposal for Phase I is trying to remove as much as possible outlying observations. With this idea in mind, the x_i observations satisfying

$$T_{i,MCD}^2 > \chi_{0.025;p}^2 \qquad (7)$$

are going to be directly discarded from the in-control sample. $\chi^2_{\alpha;p}$ stands for the $(1-\alpha)$ percentile of the chi-squared distribution with p degrees of freedom. Note that *covMcd* function in the *robustbase* package already incorporates a consistency factor and a finite sample correction factor to achieve consistency under the multivariate normal assumption [84].

Phase II: By using the criteria in (7), a subset of indexes $\{i_1, ..., i_m\} \subset \{1, 2, ..., n\}$ is obtained for a subsample of (hopefully) outlier-free data points to be considered as in-control data. Then, the sample mean $\overline{x_{-out}}$ and the sample covariance matrix S_{-out} of this subset made up with m observations are computed . A "robust phase II" chart is then derived by examining:

$$T^2_{i,-out} = (x_i - \overline{x_{-out}})' S^{-1}_{-out} (x_i - \overline{x_{-out}}), \qquad (8)$$

where x_i are the new observations to be monitored. The upper control limit is also changed to:

$$UCL_m = \frac{(m-1)^2}{m} B_{\alpha; \frac{p}{2}, \frac{m-p-1}{2}} \qquad (9)$$

(i.e., as in (5) but now only based on those m outlier-free subsample).

An observation is finally labeled as out-of-control if $T^2_{i,-out} > UCL_m$. In the next section, the proportion of observations labeled as out-control when using this approach is compared to the traditional "non-robust phase II". Distances (4) and the cut-off value (5) are directly applied in "non-robust phase II".

V. CASE STUDY

Several controlled laboratory experiments were carried out on induction motors of two kinds of specifications as shown in Table I. The motors were fed from different sources, utility supply (UT), and voltage source inverters by different manufacturers. Both motors were loaded with a magnetic powder brake. The following instrumentation and software was used to collect and analyze data: a Fluke Hall Effect probe, a PCI-6250 M DAQ board by National Instruments, LabView, MATLAB and R statistical software. The data acquisition resolution was 80 kHz. Matlab was used to process the motor line current estimating the Power Spectral Density (PSD) from the signal applying the Hanning Window in order to reduce the spectral leakage. In order to obtain a normalized PSD, the function provided by Matlab has been modified, with the amplitude of the fundamental frequency corresponding always to 0 dB.

TABLE I
SPECIFICATIONS OF THE TESTED MOTORS

Motor	Rated power (kW)	Rated voltage (V)	Rated current (A)	Rated speed (rpm)	Pole pairs
M1	0.75	3x230/400	1.9	1395	2
M2	1.1	3x230/400	2.6	1415	2

A. Broken bar diagnosis

Four rotor conditions (Table II) were tested by progressively drilling a hole into one of the rotor bars. The motor was fed from three different sources: utility supply and two VSIs by

Allen Bradley and Siemens and at different operating frequencies (35, 50 and 65 Hz.). As fault signatures, the first sideband around the main harmonic was used.

To thoroughly describe the proposed methodology, one of the tested cases is now explained in detail. In this case, a motor of type M2 is fed from a VSI by Allen Bradley (AB) with an operating frequency of 35 Hz.

Fig 1 shows the tolerance plot with the two chosen fault signatures. The tolerance ellipse obtained with a classical approach only considers as outliers the signatures from 4 tests while with the robust approach, 12 more tests are marked. This fraction of anomalous data inflates the variance-covariance matrix estimator, affecting the values of the Mahalanobis distances defining classical Hotelling's T^2 values. The effect of these outliers can be observed in Fig 2, where the control limits set without removing the outliers are shown (Fig. 2, top), and when these values have been removed (Fig. 2 bottom), obtaining a control limit more useful for diagnosis purposes in Phase II.

Fig. 3 shows the control charts in the non-robust (Fig .3 top) and robust versions (Fig. 3, bottom) when monitoring the IM. The red line in the figures corresponds to the quality control warning. If the classical approach were used, some tests belonging to the healthy motor state would be labelled as faulty ones, that is, there would be a warning although the motor is in a healthy state, while the first tests performed with an incipient fault would not be detected. On the contrary, with the robust implementation, these false alarms are eliminated and none of the healthy cases would be mislabeled. Moreover, when the fault is produced it is almost immediately detected by the control monitoring.

Table III gathers the results of the tests performed with the three voltage sources and three different operating frequencies. The last three columns show the percentage of tests that are diagnosed for each condition state with the non-robust approaches. It can be observed that the robust approaches always outperformed the non-robust one. It has to be taken into account that these percentages correspond to the corresponding condition state but, for condition states 3 and 4, all the cases are diagnosed as faulty, although in some few cases, the degree of severity is not correctly diagnosed.

TABLE II
DESCRIPTION OF THE TESTS PERFORMED. BROKEN BAR CONDITION

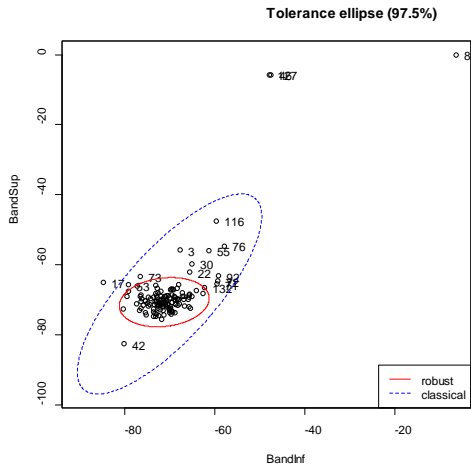| Condition state	Description	Hole depth (mm)
1	Healthy motor	0
2	Incipient fault	6.4
3	Semi-broken bar	11.7
4	Full-broken bar	17

Fig. 1. Tolerance ellipses for the first sideband around the main harmonic acquired from the healthy motor. Motor fed from an AB VSI.
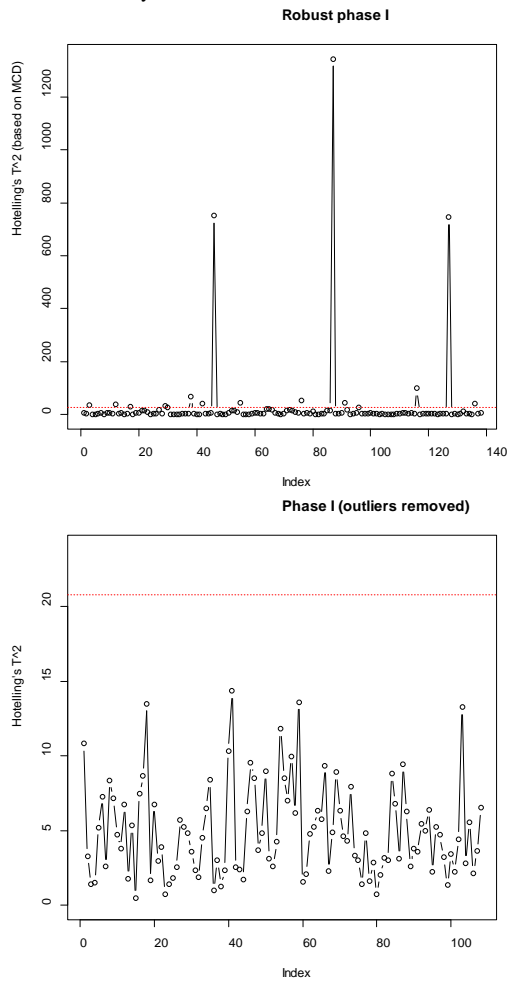

Fig. 2. Robust Phase I charts with outliers (top) and with outliers removed (bottom). The red line marks the quality control warning. When the outliers have been removed all the tests are in-control. Motor fed from an AB VSI.
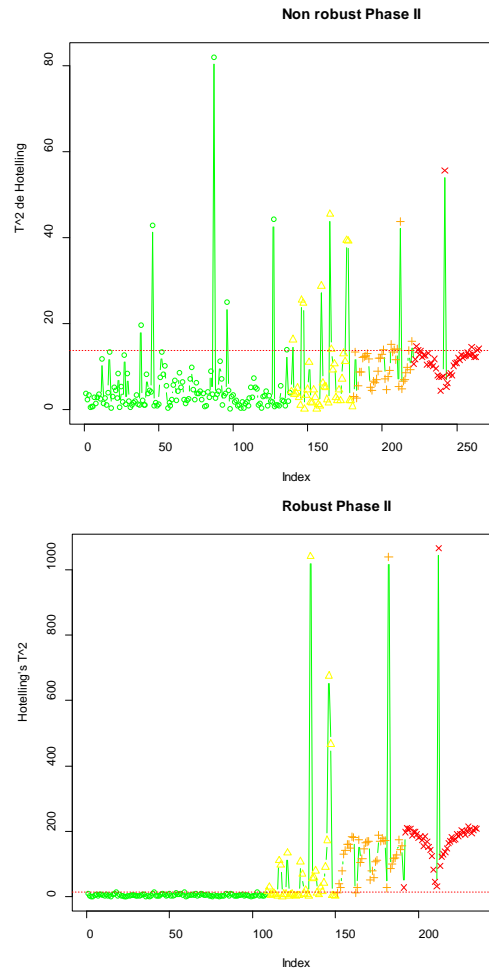

Fig. 3. Phase II charts. Non-robust (top) and robust (right) approaches. The green dots are the healthy motor tests (100 tests). The yellow, orange and red dots represent the different faulty (broken bar) condition states (Table I) (50 tests for each condition). Motor fed from an AB VSI.

TABLE III
BROKEN BAR CONDITION. RESULTS OF THE TESTS PERFORMED WITH THE NON-ROBUST AND ROBUST APPROACHES. PERCENTAGE OF DIAGNOSED TESTS FOR EACH CONDITION STATE.

Source	Operating Frequency	Method	Condition State		
			2	3	4
Allen Bradley VSI	35 Hz	Non-robust	19.05%	15.00%	13.33%
		Robust	45.24%	95.00%	100.0%
	50 Hz	Non-robust	6.52%	92.50%	97.83%
		Robust	32.61%	100.0%	100.0%
	65 Hz	Non-robust	73.17 %	97.96%	91.11%
		Robust	97.56 %	100.0%	97.78%
Siemens VSI	35 Hz	Non-robust	9.52%	85.71%	93.33%
		Robust	30.95%	100.0%	100.0%
	50 Hz	Non-robust	2.33%	69.05%	71.11%
		Robust	23.26%	90.48%	84.44%
	65 Hz	Non-robust	43.90%	45.65%	91.11%
		Robust	68.29 %	78.26%	95.56%
Utility	50 Hz	Non-robust	5.00%	11.90%	2.13%
		Robust	35.00%	85.71%	91.49%

B. Bearings.

One of the original bearings of a motor of type M1 was replaced by other bearing by SKF. The mounted open cage ball bearing belongs to the 6004 series (The characteristic q values were consulted in SKF charts). To provoke the faulty condition, a cut was made in the rolling ring.

As fault signatures, the two first sidebands (n=1, 2 in (2)) for the Fundamental Train Frequency [68] have been chosen. Figs 4 and 5 show the control chars when the motor was directly connected to the utility supply. Fig. 4 shows the Phase II control charts in the non-robust (top) and robust versions (right) when monitoring the IM running at full load. In both cases, there are no false alarms for the healthy state (green dots in Fig. 4, 10 tests). For the faulty bearing state (10 tests, red triangles in Fig. 4), all the tests are detected and diagnosed as faulty with the robust approach, but with the non-robust one, two of them are mislabeled. In the case shown in Fig. 5, the motor was running at almost no load. In this situation the non-robust approach would be completely useless since none of the faulty cases would be detected.

Fig. 6 shows the Phase II control charts in the non-robust (top) and robust versions (right) when the motor is fed from a VSI by Telemecanique with an assigned frequency of 50 Hz. running at different loads from almost no load to full load. In both cases, there are no false alarms for the healthy state (green dots, 20 tests). For the faulty bearing state (red triangles, 20 tests), all the tests are detected and diagnosed as faulty with the robust approach, but with the non-robust one, two of them are mislabeled.
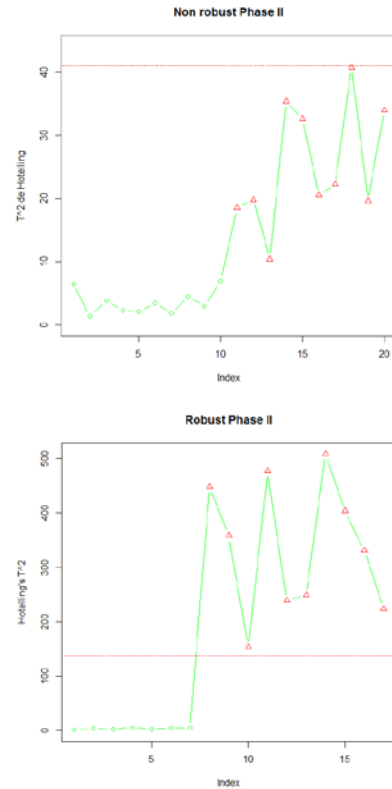

Fig. 5. Phase II charts for bearing faulty state with the motor connected directly to the utility supply and running at almost no load. Non-robust (top) and robust (right) approaches. The green dots are the healthy motor tests (10 tests). The red triangles represent the faulty bearing state (10 tests).
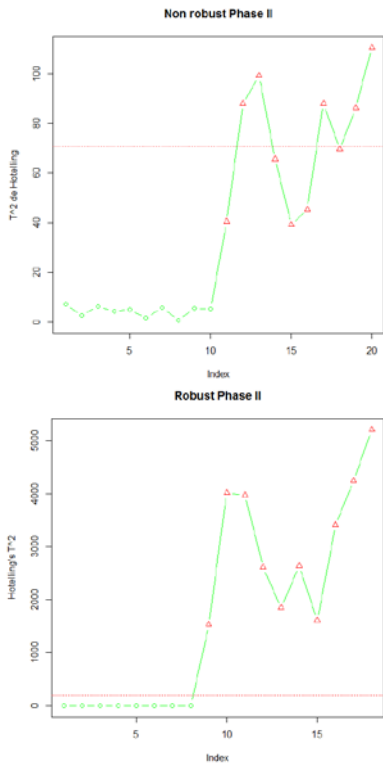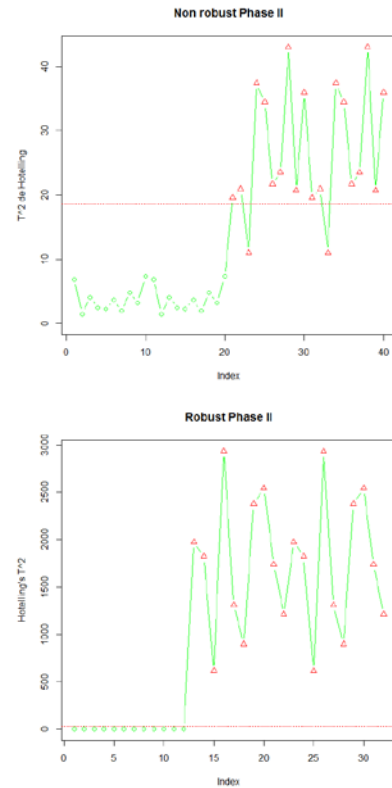

Fig. 4. Phase II charts for bearing faulty state with the motor connected directly to the utility supply and running at full load. Non-robust (top) and robust (right) approaches. The green dots are the healthy motor tests (10 tests). The red triangles represent the faulty bearing state (10 tests).

Fig. 6. Phase II charts. Motor fed from a Vart VSI at different loads from almost no load to full load . Non-robust (top) and robust (right) approaches. The green dots are the healthy motor tests (20 tests). The red triangles represent the faulty bearing state (20 tests).

C. Mixed eccentricity

An artificially created eccentricity was provoked in a motor of type M2 by putting an L-shaped iron wedge under the motor support held by a pair of cinches.

In the case shown in Fig. 7, the motor was fed from a VSI by Siemens with an assigned frequency of 65 Hz. In this case, there are no false alarms for the healthy state (green dots in Fig. 5, 20 tests). For the mixed eccentricity condition, (20 tests, yellow dots in Fig. 5), all the tests are detected and diagnosed as faulty. In this analysis, there is no difference between both approaches.
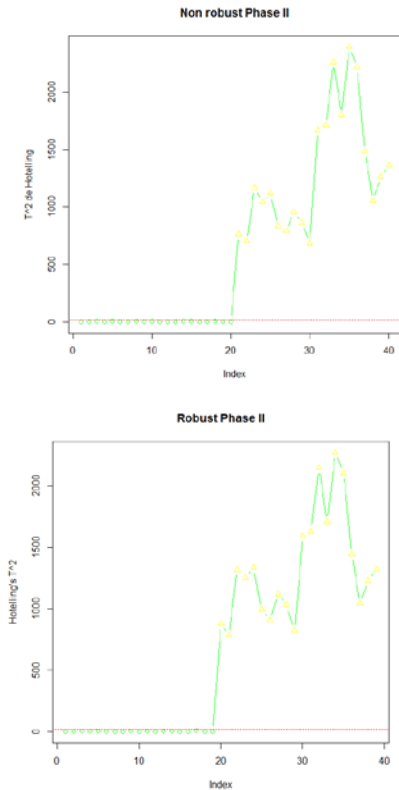

Fig. 7. Phase II chart for the mixed eccentricity case. The motor is fed from a Siemens VSI with an operating frequency of 65 Hz. The green dots are the healthy motor tests (20 tests). The yellow dots represent the mixed eccentricity condition (20 tests).

VI. Conclusions

In this work we have developed a procedure for detecting incipient faults in VSI-fed induction motors using multivariate quality control charts and shown its good performance with real motor data under different types of faults. In the case study presented, two motors of different rated power are fed from four different voltage sources, utility supply and VSIs from three different manufactures with different assigned frequencies (from 35 to 65 Hz) and running at different loads. The main advantage of our technique is that it can be implemented without having observations of the motor in a faulty condition, thus allowing for direct usage in industrial practice with a healthy motor. Another important advantage is that our procedure does not depend on the motor brand or on the feeding system.

The procedure relies on online monitoring using a multiresolution technique based on wavelet functions to detect fault signatures on the spectrum, and on a multivariate control chart that incorporates robust statistical procedures for the detection of multivariate outliers corresponding to deteriorated states. This control chart can be implemented using distribution free software, which is the third main advantage of our procedure.

References

[1] D Hyun, J Hong, SB Lee, K Kim, "Automated monitoring of airgap eccentricity for inverter-fed induction motors under standstill conditions", *IEEE Trans. Ind. Appl.*, vol. 47, no. 3, pp. 1257-1266, May-June.2011.

[2] B. Akin, U. Orguner, H.A. Toliyat and M. Rayner, "Low order PWM inverter harmonics contributions to the inverter-fed induction machine fault diagnosis," *IEEE Trans. Ind. Electron.*, vol. 55, no. 2, pp. 610–619, 2008.

[3] F. Briz, M. W. Degner, P. Garcia and A. B. Diez, "High-frequency carrier-signal voltage selection for stator winding fault diagnosis in inverter-fed ac machines," *IEEE Trans. Ind. Electron.*, vol. 55 no. 12, pp. 4181–4190, 2008.

[4] O. Duque-Perez, L. A. Garcia-Escudero, D. Morinigo-Sotelo, P. E. Gardel and M. Perez-Alonso, "Condition monitoring of induction motors fed by Voltage Source Inverters. Statistical analysis of spectral data," *Electrical Machines (ICEM), 2012 XXth International Conference on*, Marseille, 2012, pp. 2479-2484.

[5] K. Yahia, A. J. M. Cardoso, S. E. Zouzou, S. Gueddidi, "Broken rotor bars diagnosis in an induction motor fed from a frequency converter: experimental research", *Int J Syst Assur Eng Manag* vol. 3 no. 1, pp. 40–46, Jan-Mar 2012.

[6] W. F. Godoy, I. N. da Silva, A. Goedtel, R. H. C. Palácios and T. D. Lopes, "Application of intelligent tools to detect and classify broken rotor bars in three-phase induction motors fed by an inverter," in *IET Electric Power Applications*, vol. 10, no. 5, pp. 430-439, 5 2016.

[7] S. Altaf, A. Al-Anbuky and H. GholamHosseini, "Fault diagnosis in a distributed motor network using Artificial Neural Network," Power Electronics, Electrical Drives, Automation and M*otion (SPEEDAM), 2014 International Symposium on*, Ischia, 2014, pp. 190-197.

[8] S. S. Refaat, H. Abu-Rub, M. S. Saad and A. Iqbal, "Open and closed-loop motor control system with incipient broken rotor bar fault detection using current signature," *IECON 2014 - 40th Annual Conference of the IEEE Industrial Electronics Society*, Dallas, TX, 2014, pp. 774-780.

[9] H. Singh, M. Seera and M. Z. Abdullah, "Detection and diagnosis of broken rotor bars and eccentricity faults in induction motors using the Fuzzy Min-Max neural network," *Neural Networks (IJCNN), The 2013 International Joint Conference on*, Dallas, TX, 2013, pp. 1-5.

[10] T. Boukra, A. Lebaroud and G. Clerc, "Statistical and Neural-Network Approaches for the Classification of Induction Machine Faults Using the Ambiguity Plane Representation," in *IEEE Transactions on Industrial Electronics*, vol. 60, no. 9, pp. 4034-4042, Sept. 2013.

[11] A. Sadeghian, Z. Ye and B. Wu, "Online Detection of Broken Rotor Bars in Induction Motors by Wavelet Packet Decomposition and Artificial Neural Networks," in *IEEE Transactions on Instrumentation and Measurement*, vol. 58, no. 7, pp. 2253-2263, July 2009.

[12] B. Ayhan, M. Y. Chow and M. H. Song, "Multiple Discriminant Analysis and Neural-Network-Based Monolith and Partition Fault-Detection Schemes for Broken Rotor Bar in Induction Motors," in *IEEE Transactions on Industrial Electronics*, vol. 53, no. 4, pp. 1298-1308, June 2006.

[13] Woei Wan Tan and Hong Huo, "A generic neurofuzzy model-based approach for detecting faults in induction motors," in *IEEE Transactions on Industrial Electronics*, vol. 52, no. 5, pp. 1420-1427, Oct. 2005.

[14] Kyusung Kim, A. G. Parlos and R. Mohan Bharadwaj, "Sensorless fault diagnosis of induction motors," in *IEEE Transactions on Industrial Electronics*, vol. 50, no. 5, pp. 1038-1051, Oct. 2003.

[15] W. Sun, S. Shao, R. Zhao, R. Yan, X. Zhang, X. Chen, "A sparse auto-encoder-based deep neural network approach for induction motor faults classification", *Measurement*, vol. 89, pp. 171–178, July 2016.

[16] E. Cabal-Yepez, M. Valtierra-Rodriguez, R.J. Romero-Troncoso, A. Garcia-Perez, R.A. Osornio-Rios, H. Miranda-Vidales, R. Alvarez-Salas, "FPGA-based entropy neural processor for online detection of multiple combined faults on induction motors", *Mechanical Systems and Signal Processing*, vol. 30, pp. 123-130, July 2012

[17] M. Hernandez-Vargas, E. Cabal-Yepez, A. Garcia-Perez, "Real-time SVD-based detection of multiple combined faults in induction motors", *Computers & Electrical Engineering*, vol. 40, no. 7, pp. 2193-2203, October 2014.

[18] Z. Ye, A. Sadeghian, B. Wu, "Mechanical fault diagnostics for induction motor with variable speed drives using Adaptive Neuro-fuzzy Inference", *Electric Power Systems Research*, vol. 76, no. 9–10, pp. 742-752, June 2006.

[19] T. Han, B. Yang, Z. Yin, "Feature-based fault diagnosis system of induction motors using vibration signal", *Journal of Quality in Maintenance Engineering* vol. 13 no. 2, pp. 163-175, 2007

[20] P. Gardel, D. Morinigo-Sotelo, O. Duque-Perez, M. Perez-Alonso and L. A. Garcia-Escudero, "Neural network broken bar detection using time domain and current spectrum data," *Electrical Machines (ICEM), 2012 XXth International Conference on*, Marseille, 2012, pp. 2492-2497.

[21] M. Seera and C. P. Lim, "Online Motor Fault Detection and Diagnosis Using a Hybrid FMM-CART Model," in *IEEE Transactions on Neural Networks and Learning Systems*, vol. 25, no. 4, pp. 806-812, April 2014.

[22] V. N. Ghate and S. V. Dudul, "Cascade Neural-Network-Based Fault Classifier for Three-Phase Induction Motor," in *IEEE Transactions on Industrial Electronics*, vol. 58, no. 5, pp. 1555-1563, May 2011.

[23] X. Huang, T. G. Habetler and R. G. Harley, "Detection of Rotor Eccentricity Faults in a Closed-Loop Drive-Connected Induction Motor Using an Artificial Neural Network," in *IEEE Transactions on Power Electronics*, vol. 22, no. 4, pp. 1552-1559, July 2007.

[24] S. Wu and T. W. S. Chow, "Induction machine fault detection using SOM-based RBF neural networks," in *IEEE Transactions on Industrial Electronics*, vol. 51, no. 1, pp. 183-194, Feb. 2004.

[25] V.N. Ghate, S.V. Dudul, "Optimal MLP neural network classifier for fault detection of three phase induction motor", *Expert Systems with Applications*, vol. 37, no. 4, pp. 3468-3481, April 2010.

[26] H. L. Schmitt, L. R. B. Silva, P. R. Scalassara and A. Goedtel, "Bearing fault detection using relative entropy of wavelet components and artificial neural networks," *Diagnostics for Electric Machines, Power Electronics and Drives (SDEMPED), 2013 9th IEEE International Symposium on*, Valencia, 2013, pp. 538-543.

[27] M. D. Prieto, G. Cirrincione, A. G. Espinosa, J. A. Ortega and H. Henao, "Bearing Fault Detection by a Novel Condition-Monitoring Scheme Based on Statistical-Time Features and Neural Networks," in *IEEE Transactions on Industrial Electronics*, vol. 60, no. 8, pp. 3398-3407, Aug. 2013.

[28] H. C. Cho, J. Knowles, M. S. Fadali and K. S. Lee, "Fault Detection and Isolation of Induction Motors Using Recurrent Neural Networks and Dynamic Bayesian Modeling," in *IEEE Transactions on Control Systems Technology*, vol. 18, no. 2, pp. 430-437, March 2010.

[29] M. S. Ballal, Z. J. Khan, H. M. Suryawanshi and R. L. Sonolikar, "Adaptive Neural Fuzzy Inference System for the Detection of Inter-Turn Insulation and Bearing Wear Faults in Induction Motor," in *IEEE Transactions on Industrial Electronics*, vol. 54, no. 1, pp. 250-258, Feb. 2007.

[30] B. Liang, S.D. Iwnicki, Y. Zhao, "Application of power spectrum, cepstrum, higher order spectrum and neural network analyses for induction motor fault diagnosis", *Mechanical Systems and Signal Processing*, vol. 39 no. 1–2, pp 342-360. August–September 2013.

[31] P.K. Kankar, S.C. Sharma, S.P. Harsha, "Fault diagnosis of ball bearings using machine learning methods", *Expert Systems with Applications*, vol. 38, no. 3, pp. 1876-1886, March 2011.

[32] J. Zarei, "Induction motors bearing fault detection using pattern recognition techniques", *Expert Systems with Applications*, vol. 39, no. 1, pp. 68-73, January 2012.

[33] Z. Xu, J. Xuan, T. Shi, B. Wu, Y. Hu, "Application of a modified fuzzy ARTMAP with feature-weight learning for the fault diagnosis of bearing", *Expert Systems with Applications*, vol. 36, no. 6, pp. 9961-9968, August 2009.

[34] F. Jia, Y. Lei, J. Lin, X. Zhou, N. Lu, "Deep neural networks: A promising tool for fault characteristic mining and intelligent diagnosis of rotating machinery with massive data", *Mechanical Systems and Signal Processing*, vol. 72–73, pp. 303-315, May 2016.

[35] S. Hamdani, H. Mezerreg, B. Boutikar, N. Lahcene, O. Touhami and R. Ibtiouen, "Rotor fault diagnosis in a Squirrel-Cage Induction Machine using support vector machine," *Electrical Machines (ICEM), 2012 XXth International Conference on*, Marseille, 2012, pp. 1817-1822.

[36] Y. K. Moorthy, P. S. Chandran and S. Rishidas, "Motor current signature analysis by multi-resolution methods using Support Vector Machine," *Recent Advances in Intelligent Computational Systems (RAICS), 2011 IEEE*, Trivandrum, 2011, pp. 096-101.

[37] A. Widodo, B.S. Yang, T. Han, "Combination of independent component analysis and support vector machines for intelligent faults diagnosis of induction motors", *Expert Systems with Applications*, vol. 32, no. 2, pp. 299-312, February 2007.

[38] D. Matić, F. Kulić, M. Pineda-Sánchez, I. Kamenko, "Support vector machine classifier for diagnosis in electrical machines: Application to broken bar", *Expert Systems with Applications*, vol. 39, no. 10, pp. 299-312, August 2012, pp. 299-312.

[39] H. Keskes, A. Braham, Z. Lachiri, "Broken rotor bar diagnosis in induction machines through stationary wavelet packet transform and multiclass wavelet SVM", *Electric Power Systems Research*, vol. 97, pp. 151-157, April 2013.

[40] H. O. Vishwakarma, K. S. Sajan, B. Maheshwari and Y. D. Dhiman, "Intelligent bearing fault monitoring system using support vector machine and wavelet packet decomposition for induction motors," *Power and Advanced Control Engineering (ICPACE), 2015 International Conference on*, Bangalore, 2015, pp. 339-343.

[41] J. Zarei, M. M. Arefi and H. Hassani, "Bearing fault detection based on interval type-2 fuzzy logic systems for support vector machines," *Modeling, Simulation, and Applied Optimization (ICMSAO), 2015 6th International Conference on*, Istanbul, 2015, pp. 1-6.

[42] M. Barakat, D. Lefebvre, M. Khalil, O. Mustapha and F. Druaux, "BSP-BDT classification technique: Application to rolling elements bearing," *2010 Conference on Control and Fault-Tolerant Systems (SysTol)*, Nice, 2010, pp. 654-659.

[43] P. Konar, P. Chattopadhyay, "Bearing fault detection of induction motor using wavelet and Support Vector Machines (SVMs)", *Applied Soft Computing*, vol. 11, no. 6, pp. 4203-4211, September 2011.

[44] S. Ben Salem, K. Bacha, A. Chaari, "Support vector machine based decision for mechanical fault condition monitoring in induction motor using an advanced Hilbert-Park transform", *ISA Transactions*, vol. 51, no. 5, pp. 566-572, September 2012.

[45] C. Rajeswari, B. Sathiyabhama, S. Devendiran, K. Manivannan, "Bearing Fault Diagnosis using Wavelet Packet Transform, Hybrid PSO and Support Vector Machine", *Procedia Engineering*, vol. 97, pp. 1772-1783, 2014.

[46] X. Zhang, J. Zhou, "Multi-fault diagnosis for rolling element bearings based on ensemble empirical mode decomposition and optimized support vector machines", *Mechanical Systems and Signal Processing*, vol. 41, no. 1–2, pp. 127-140, December 2013.

[47] Xu Li, A. Zheng, X. Zhang, C. Li, Li Zhang, "Rolling element bearing fault detection using support vector machine with improved ant colony optimization", *Measurement*, vol. 46, no. 8, pp. 2726-2734, October 2013.

[48] S. Abbasion, A. Rafsanjani, A. Farshidianfar, N. Irani, "Rolling element bearings multi-fault classification based on the wavelet denoising and support vector machine", *Mechanical Systems and Signal Processing*, vol. 21, no. 7, pp. 2933-2945, October 2007.

[49] K. Zhu, X. Song, D. Xue, "A roller bearing fault diagnosis method based on hierarchical entropy and support vector machine with particle swarm optimization algorithm", *Measurement*, vol. 47, pp. 669-675, January 2014.

[50] C. Delpha, H. Chen and D. Diallo, "SVM based diagnosis of inverter fed induction machine drive: A new challenge," *IECON 2012 - 38th Annual Conference on IEEE Industrial Electronics Society*, Montreal, QC, 2012, pp. 3931-3936.

[51] A. Bouguerne, A. Lebaroud, A. Medoued and A. Boukadoum, "Classification of induction machine faults by K-nearest neighbor," *Electrical and Electronics Engineering (ELECO), 2011 7th International Conference on*, Bursa, 2011, pp. I-363-I-366.

[52] M. Farajzadeh-Zanjani, R. Razavi-Far, M. Saif, J. Zarei and V. Palade, "Diagnosis of Bearing Defects in Induction Motors by Fuzzy-Neighborhood Density-Based Clustering," *2015 IEEE 14th International Conference on Machine Learning and Applications (ICMLA)*, Miami, FL, 2015, pp. 935-940.

[53] H. W. Peng and P. J. Chiang, "Control of mechatronics systems: Ball bearing fault diagnosis using machine learning techniques," *Control Conference (ASCC), 2011 8th Asian*, Kaohsiung, 2011, pp. 175-180.

[54] S. P. Santos and J. A. F. Costa, "A Comparison between Hybrid and Non-hybrid Classifiers in Diagnosis of Induction Motor Faults," *Computational Science and Engineering, 2008. CSE '08. 11th IEEE International Conference on*, Sao Paulo, 2008, pp. 301-306.

[55] S. Ergin, S. Tezel and M. B. Gulmezoglu, "DWT-based fault diagnosis in induction motors by using CVA," *Innovations in Intelligent Systems and Applications (INISTA), 2011 International Symposium on*, Istanbul, 2011, pp. 129-132.

[56] G. Georgoulas, M.O. Mustafa, I.P. Tsoumas, J.A. Antonino-Daviu, V. Climente-Alarcon, C.D. Stylios, G. Nikolakopoulos, "Principal Component Analysis of the start-up transient and Hidden Markov Modeling for broken rotor bar fault diagnosis in asynchronous machines", *Expert Systems with Applications*, vol. 40, no. 17, pp. 7024-7033, December 2013.

[57] A. Soualhi, G. Clerc, H. Razik and A. Lebaroud, "Fault detection and diagnosis of induction motors based on hidden Markov model," *Electrical Machines (ICEM), 2012 XXth International Conference on*, Marseille, 2012, pp. 1693-1699.

[58] S. Yusuf, D. J. Brown, A. Mackinnon and R. Papanicolaou, "Fault classification improvement in industrial condition monitoring via Hidden Markov Models and Naïve Bayesian modeling," *Industrial Electronics and Applications (ISIEA), 2013 IEEE Symposium on*, Kuching, 2013, pp. 75-80.

[59] V. Sugumaran, K.I. Ramachandran, "Automatic rule learning using decision tree for fuzzy classifier in fault diagnosis of roller bearing", *Mechanical Systems and Signal Processing*, vol. 21, no. 5, pp. 2237-2247, July 2007.

[60] M. Seera, C.P. Lim, S. Nahavandi, C.K. Loo, "Condition monitoring of induction motors: A review and an application of an ensemble of hybrid intelligent model", *Expert Systems with Applications*, vol. 41, no. 10, pp. 4891-4903, August 2014.

[61] C.T. Yiakopoulos, K.C. Gryllias, I.A. Antoniadis, "Rolling element bearing fault detection in industrial environments based on a K-means clustering approach", *Expert Systems with Applications*, vol. 38, no. 3, pp. 2888-2911, March 2011.

[62] X. Jin, F. Yuan, T.W.S. Chow, M. Zhao, "Weighted local and global regressive mapping: A new manifold learning method for machine fault classification", *Engineering Applications of Artificial Intelligence*, vol. 30, pp. 118–128, April 2014.

[63] A. Bellini, F. Filippetti, C. Tassoni, G.A. Capolino, "Advances in diagnostic techniques for induction machines," *IEEE Trans. Ind. Electron.*, vol. 55 no. 12, pp. 4109–4126, 2008.

[64] F. Filippetti, A. Bellini and G. A. Capolino, "Condition monitoring and diagnosis of rotor faults in induction machines: State of art and future perspectives," *Electrical Machines Design Control and Diagnosis (WEMDCD), 2013 IEEE Workshop on*, Paris, 2013, pp. 196-209.

[65] O. Duque-Perez, L.A. Garcia-Escudero, D. Morinigo-Sotelo, P.E. Gardel, M. Perez-Alonso, "Analysis of Fault Signatures for the Diagnosis of Induction Motors fed by Voltage Source Inverters using ANOVA and Additive Models", *Electric Power Systems Research*. Vol 121, pp. 1-13, 2015.

[66] M. Fernandez-Temprano, P.E. Gardel-Sotomayor, O. Duque-Perez ; D. Morinigo-Sotelo, "Broken bar condition monitoring of an induction motor under different supplies using a linear discriminant analysis", *Diagnostics for Electric Machines, Power Electronics and Drives (SDEMPED), 2013 9th IEEE International Symposium on*, pp. 162–168.

[67] M. E. H. Benbouzid and G. B. Kliman, "What stator current processing-based technique to use for induction motor rotor faults diagnosis?," in *IEEE Transactions on Energy Conversion*, vol. 18, no. 2, pp. 238-244, June 2003.

[68] O. Duque, M. Perez and D. Morinigo, "Detection of Bearing Faults in Cage Induction Motors Fed by Frequency Converter using Spectral Analysis of Line Current," *IEEE International Conference on Electric Machines and Drives, 2005*, San Antonio, TX, 2005, pp. 17-22.

[69] D.C. Montgomery, *Introduction to Statistical Quality Control*, 7th Edition, Ed. Wiley 2012.

[70] G. Hanrahan, *Environmental Chemometrics: Principles and Modern Applications*, Ed. CRC Press, 2008.

[71] E.B. Howington, "Robust Monitoring of Contaminated Multivariate Data", *Advances in Decision Sciences*, vol. 2013, Article ID 9615012, 2013.

[72] R.L. Mason and J.C. Young, *Multivariate Statistical Process Control with Industrial Applications*. Ed. ASA/SIAM, 2002.

[73] R.L. Mason, N.D. Tracy and J.C. Young, "Decomposition of T^2 for multivariate control chart interpretation". *Journal of Quality Technology*, vol. 27, pp. 109–119, 1995.

[74] D.M. Hawkings, "Multivariate quality control based on regression-adjusted variables". *Technometrics* vol. 33, pp.61–75, 1993.

[75] N. Das and V. Prakash, "Interpreting the out-of-control signal in multivariate control chart — a comparative study". *Int J Adv Manuf Technol*, vol. 37, pp. 966–979, 2008.

[76] S. Vidal-Puig and A. Ferre, "A comparative study of different methodologies for fault diagnosis in multivariate quality control. Communications in *Statistics-Simulation and Computation*, vol. 43, pp.986–1005, 2014.

[77] E. Alfaro, J.L. Alfaro, M. Gámez and N. García, "A Comparison of Different Classification Techniques to Determine the Change Causes in Hotelling's T^2 Control Chart. *Qual. Reliab. Engng. Int*. 2015, vol. 31, pp. 1255–1263, 2015.

[78] R.E. Schapire and Y. Freund, *Boosting: Foundations and Algorithms*. The MIT Press, 2012.

[79] Rousseeuw P. J. and Leroy, A. M. *Robust Regressions and Outlier Detection*. Wiley, New York, 1987.

[80] J.A. Vargas, "Robust Estimation in Multivariate Control Charts for Individual Observation". *Journal of Quality Technology*. vol. 35, no. 4, 2003.

[81] W.A. Jensen, J.B. Birch, and W.H. Woodall, "High Breakdown Estimation for Phase I Multivariate Control Charts", *Quality and Reliability Engineering International*, vol. 23, pp. 615-629, 2007.

[82] J.L. Alfaro and J.F. Ortega, "A robust alternative to Hotelling's T2 control chart using trimmed estimators", *Quality and Reliability Engineering International*, vol. 24, pp. 601-611, 2008.

[83] G. Stefatos and A. B. Hamza, "Fault detection using robust multivariate control chart", *Expert Systems with Applications*, vol. 36, pp. 5888-5894, 2009.

[84] G. Pison, S. Van Aelst and G. Willems, "Small Sample Corrections for LTS and MCD", *Metrika*, vol. 55, pp. 111–123, 2002.